

# Self-Crystallization of C<sub>70</sub> Cubes and Remarkable Enhancement of Photoluminescence\*\*

Chibeom Park, Eunjin Yoon, Masaki Kawano, Taiha Joo, and Hee Cheul Choi\*

Light emission from organic molecular systems is one of the essential properties for the development of next-generation cost-effective, light, flexible, and large-scale electronic and optoelectronic devices.<sup>[1,2]</sup> Because the light emission mediated by exciton recombination requires a specific energy band gap, highly conjugated organic molecules in the form of crystalline structures have been studied intensively for this purpose,<sup>[3,4]</sup> and diverse strategies have been developed for the synthesis of highly conjugated organic and polymeric molecules with geometrically well-defined crystal shapes,<sup>[5,6]</sup> by which their optical properties can be modulated.

Fullerenes, one of the most popular types of highly conjugated organic molecules, have been studied mainly for their semiconducting<sup>[7]</sup> and superconducting<sup>[8,9]</sup> properties, which result from the discrete HOMO–LUMO band structure as well as the facile doping effect on low-lying energy levels of empty orbitals, into which extra electrons are readily accommodated. In contrast, their optical emission properties have scarcely attracted any attention because of the low exciton population for radiative recombination in fullerene molecules.<sup>[10]</sup> However, fullerene molecules are still believed to have much potential in terms of their optical properties, as indicated by recent observations of abnormally increased fluorescence from self-aggregated molecules that have intrinsically low emitting power when they exist in an

ensemble state in solution or powder phases. For example, Hara and co-workers reported that an asymmetric disulfide compound in which a photoisomerizable azobenzene unit was coupled to a biphenyl fluorophore generally showed negligible fluorescence, but that the photoinduced aggregation of the fluorophores led to remarkably increased fluorescence intensity.<sup>[11]</sup> The Tang and Park research groups have reported similar phenomena brought about by so-called aggregation-induced emission (AIE)<sup>[12,13]</sup> or crystallization-induced emission enhancement (CIEE).<sup>[14,15]</sup> In the case of fullerenes, changes in the photophysical properties of C<sub>60</sub> and C<sub>70</sub> upon aggregation have also been investigated: both absorption and fluorescence spectra were gradually modulated as the degree of aggregation was systematically changed.<sup>[16–21]</sup> However, such changes in fluorescence properties were mainly observed for random aggregates, no detailed crystal structures of which are available.

Herein we report that C<sub>70</sub> molecules undergo self-crystallization into high-definition cube-shaped crystals in the solution phase at room temperature. As a result of their high crystallinity with sharp edges, C<sub>70</sub> cube crystals display enhanced fluorescence. Such fluorescence has not been observed from C<sub>70</sub> in either powders or bulk crystals under ambient conditions at room temperature. The synthesis of C<sub>70</sub> cube crystals in the solution phase was inspired by recent discoveries of “geometrically defined” fullerene structures obtained through 1) precipitation in a mixture of solvents, 2) drop drying, and 3) vapor transport. In the case of the precipitation method, fullerenes spontaneously aggregate in two-solvent mixtures containing good and poor solvents for fullerenes, and their geometrical structures are determined by the type and shape of the solvents.<sup>[22,23]</sup> A drop-drying process with a single good solvent also resulted in various C<sub>60</sub> structures, such as spherical particles, wires, and hexagonal disks, the geometries of which were determined selectively according to the type of solvent used.<sup>[24–26]</sup> Both processes in the solution phase lead to the inclusion of solvent molecules in the final fullerene crystals; however, solvent-free and highly crystalline C<sub>60</sub> hexagonal disks were also obtained by a vapor-transport process.<sup>[27]</sup> In our current study, we synthesized unprecedented C<sub>70</sub> cube crystals by precipitation from a mixture of the good solvent mesitylene and the poor solvent isopropyl alcohol (IPA).

We first attempted the precipitation method for the synthesis of C<sub>70</sub> cube crystals in a solvent mixture composed of mesitylene and IPA. C<sub>70</sub> powder was dissolved in mesitylene, and IPA was slowly added to the resulting solution to form an immiscible liquid–liquid interface. The mixture was then agitated by manual shaking and kept at room temperature without any further agitation for 24 h. A fine black precipitate

[\*] C. Park, Prof. Dr. H. C. Choi

Department of Chemistry and Division of Advanced Materials Science, Pohang University of Science and Technology  
San 31, Hyoja-Dong, Nam-Gu, Pohang, 790-784 (Korea)  
Fax: (+82) 54-279-3399  
E-mail: choihc@postech.edu  
Homepage: <http://www.postech.ac.kr/chem/nmrl>

E. Yoon, Prof. Dr. T. Joo

Department of Chemistry  
Pohang University of Science and Technology  
Prof. Dr. M. Kawano  
Division of Advanced Materials Science  
Pohang University of Science and Technology

[\*\*] This research was supported by National Research Foundation of Korea (NRF) grants funded by MEST (2010-00285, 2008-04306, 2007-8-1158, 2005-01325), KOSEF (through the EPB center; R11-2008-052-02000), and the Ministry of Health, Welfare & Family Affairs (A0900062), and by the Korean Research Foundation (MOEHRD, KRF-2005-00513103). H.C.C. thanks the World Class University (WCU) program (R31-2008-000-10059-0). We thank D. Y. Noh and K.-J. Kim at the 5C2 beamline of the Pohang Accelerator Laboratory (PAL) for XRD measurement, N. Won for fluorescence microscope imaging, and D. M. Kim and Y.-G. Ko for TGA measurement.



Supporting information for this article is available on the WWW under <http://dx.doi.org/10.1002/anie.201005076>.

started to appear after approximately 3 h. When we collected the final black precipitate, we found crystals the shape of rectangular prisms with high-definition edges. However, the  $C_{70}$  cube crystals showed quite a broad size distribution, which may be due to inhomogeneous nucleation of  $C_{70}$  molecules during precipitation (see Figure S1 in the Supporting Information). To increase the size homogeneity, we applied brief ultrasonication for the first 30 s after the rapid addition (in 3–4 s) of IPA to the solution of  $C_{70}$  in mesitylene. The color of the mixture changed from light reddish brown to dark blackish brown within the first 30 s of the reaction, as observed for the reaction without ultrasonication. This observation implies that nucleation for the self-crystallization of  $C_{70}$  occurs almost instantaneously. Although the growth rate was not affected significantly by ultrasound treatment, as indicated by the color change of the solution, the size distribution and shape uniformity of the  $C_{70}$  cubes were improved enormously, with an average size of  $2.05\ \mu\text{m}$  (Figure 1; the  $C_{70}$  crystals shown were obtained from a 1:4 (v/v) mixture of the  $C_{70}$ /mesitylene solution ( $0.2\ \text{mg mL}^{-1}$ ) and IPA). This observation indicates that the nucleation step occurs more homogeneously with the assistance of ultrasonication, whereas the process without ultrasonication allows random nucleation only at the interface of two liquids through slow diffusion (Figure 2). An optical microscopic image in the bright-field reflection mode revealed a shiny and yellowish metallike  $C_{70}$  surface, which implies that the  $C_{70}$  surface is highly populated with free electrons (Figure 1 c).

We believe the key factor for  $C_{70}$  cube formation to be the formation of local mesitylene cavities, which are instantaneously generated when IPA is added to the  $C_{70}$ /mesitylene solution. Owing to the low solubility of  $C_{70}$  in IPA, the local concentration of  $C_{70}$  in the mesitylene cavities is increased, and therefore instant nucleation of  $C_{70}$  occurs in the mesitylene cavities. This mixed-solvent-mediated nucleation phenomenon is similar to the traditional recrystallization process and the synthesis of various self-crystallized  $C_{60}$  structures. Once  $C_{70}$  molecules are localized in the cavity of the good solvent mesitylene, which is surrounded by IPA, mesitylene guides  $C_{70}$  molecules to self-crystallize into cubes. To evaluate the influences of mesitylene and IPA on the formation of  $C_{70}$  cubes, we performed control experiments by

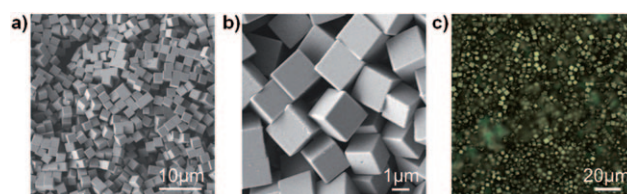


**Figure 1.** Homogeneous  $C_{70}$  cube crystals. a) Low- and b) high-magnification SEM images of  $C_{70}$  cube crystals; c) bright-field optical microscope image.

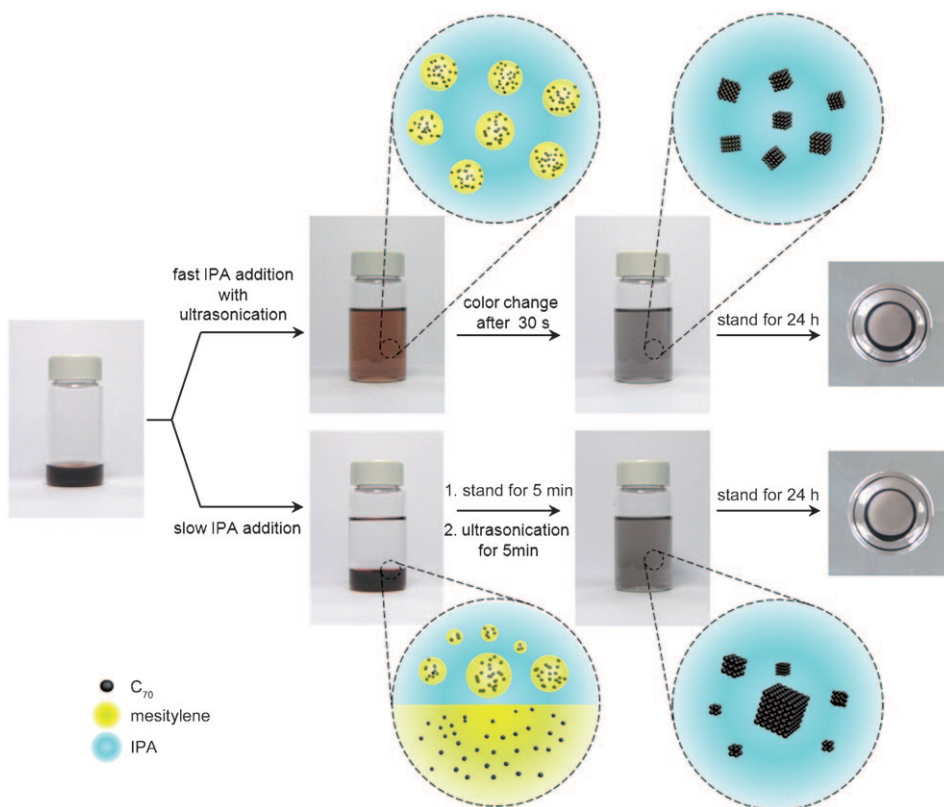


**Figure 2.** Schematic representation of the precipitation method for the self-crystallization of  $C_{70}$  cubes. The two right-most images were taken from the bottom of the vials; the black rings are precipitates of  $C_{70}$  cubes.

systematically changing 1) the concentration of  $C_{70}$  in mesitylene from 0.1 to  $0.4\ \text{mg mL}^{-1}$  and 2) the volume ratio of the  $C_{70}$ /mesitylene solution to IPA from 1:1 to 1:4. Similar cube-shaped crystals with homogeneous size distributions were obtained under almost all conditions, with the exception of the stacked pyramidal crystals formed from a 1:1 mixture of the  $C_{70}$ /mesitylene ( $0.1\ \text{mg mL}^{-1}$ ) solution and IPA (Figure 3). Meanwhile, the average size of the  $C_{70}$  cubes gradually decreased as both the amount of IPA and the concentration of  $C_{70}$  in the starting solution increased. These results support the hypothesis that the addition of IPA induces local cavities of mesitylene in which  $C_{70}$  molecules are localized and their self-crystallization guided. Since the size of the cavity should become smaller as the amount of IPA is increased, the average size of the resulting cube crystal is also smaller. The decrease in the average size as the  $C_{70}$  concentration is

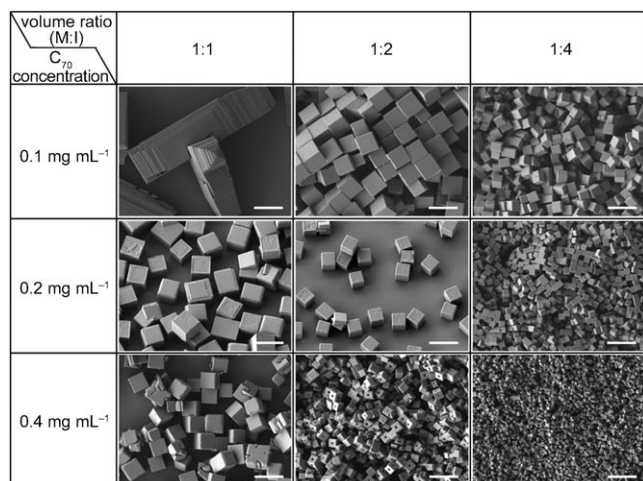


**Figure 3.** Dependence of the size and morphology of  $C_{70}$  cubes on the solution composition. The scale bars in the images are 10  $\mu\text{m}$ ; M and I stand for the  $C_{70}$ /mesitylene solution and IPA, respectively.

increased can be explained by the increased number of nucleation sites, as exemplified by various syntheses of semiconductor quantum-dot particles.

To further confirm the role of IPA as a favorable “poor” solvent during the precipitation process, we attempted the same reactions with methanol, ethanol, and acetone instead of IPA. Self-crystallized  $C_{70}$  crystals were also obtained from these solvent systems, but the edges were not sharp, and the size distribution was quite broad even with ultrasonication. Thus, the combination of mesitylene and IPA provided the most favorable self-crystallization environment for  $C_{70}$  (see Figure S2 in the Supporting Information). Although IPA affords cavity room for crystallization, it is mesitylene that directly causes the crystallization of  $C_{70}$  molecules into cube crystals, since random  $C_{70}$  crystal morphologies were obtained when mesitylene was replaced with toluene, *m*-xylene, and *m*-dichlorobenzene (see Figure S3 in the Supporting Information), in agreement with previous results.<sup>[28,29]</sup>

Whether or not mesitylene and IPA were included in the  $C_{70}$  crystals was a point of keen interest, so we investigated the crystals by gas chromatography–mass spectrometry (GC–MS) and thermal gravimetric analysis (TGA) for the presence of the solvents. For GC–MS analysis,  $C_{70}$  cubes were dissolved in  $\text{CCl}_4$  and injected into the GC–MS instrument.<sup>[26]</sup> Two components were separated at 1.82 and 6.91 min by GC (see Figure S4a in the Supporting Information) and identified as  $\text{CCl}_4$  and mesitylene, respectively, from the MS spectra (see Figure S4b,c in the Supporting Information). Notably, the poor solvent IPA was not detected, which implies that IPA indeed only induces local cavities of  $C_{70}$ /mesitylene without direct involvement in the crystallization. The ratio of  $C_{70}$  to mesitylene in a  $C_{70}$  cube was estimated by TGA conducted in a nitrogen atmosphere (see the Supporting Information for the preparation of the sample for TGA). A significant weight decrease occurred at 80 °C, and the weight continued to decrease until the temperature reached about 230 °C (see Figure S4d in the Supporting Information). The final weight loss of 22.7% due to the removal of mesitylene indicates that

the ratio of mesitylene to  $C_{70}$  is 2.05, as calculated by dividing the weight change by the molecular weight of each component. According to the GC–MS and TGA results, the chemical formula of a  $C_{70}$  cube crystal is  $C_{70}\cdot(\text{mesitylene})_2$ , which agrees well with a previous result for a bulk  $C_{70}$ /mesitylene crystal.<sup>[30]</sup>

The detailed crystal structure of the  $C_{70}$  cube was modeled on the basis of single-crystal X-ray diffraction data. To obtain  $C_{70}$  cube crystals large enough for X-ray crystallography, we used a classical liquid–liquid diffusion (LLD) process<sup>[31,32]</sup> (see the Experimental Section). The size of the crystals formed by the LLD process varied from 10 to 100  $\mu\text{m}$ ; however, these crystals also had a cube or rectangular-prism shape. With a selected cube crystal, we first attempted to collect single-crystal X-ray diffraction data at room temperature, but failed to obtain a reasonable amount of data. This difficulty seemed to be due to the thermal motion of  $C_{70}$  molecules positioned at lattice points; the motion of these molecules increases the Debye–Waller factor, as in the case of single crystals of  $C_{60}$ .<sup>[33]</sup> Hence, the data was collected at 90 K, and the crystal structure was resolved.<sup>[34]</sup> The crystal structure of  $C_{70}\cdot(\text{mesitylene})_2$  was determined to have a cubic unit cell ( $a = b = c = 10.4774(8)$  Å). On the basis of a careful Laue group check, a space group  $P\bar{4}3m$  was selected.<sup>[35]</sup> The approximate position of  $C_{70}$  was determined by using a rigid-group model, and it was converged to the center of the unit cell. Because of 24 symmetry operations, symmetry-related  $C_{70}$  molecules form spherical electron density. Difference Fourier synthesis generated several electron-density peaks corresponding to mesitylene molecules positioned near each corner of the unit cell. These positions are related to the interstitial sites available in a  $C_{70}$  cube crystal and are analogous to the positions occupied by solvent molecules in 1D and 2D  $C_{60}$  and  $C_{70}$  crystals formed through the mediation of different types of solvent.<sup>[22,24,26]</sup> Refinement based on the use of two independent mesitylene molecules converged to a final *R* factor of 20%. The  $C_{70}$  molecule is located in the center of the unit cell, and two mesitylene molecules occupy each corner with a partial occupancy factor (Figure 4). There is no particularly short contact between  $C_{70}$  and mesitylene.

Since these results correspond to the crystal structure of  $C_{70}$  as it exists at low temperature, we analyzed the  $C_{70}$  cubes again at room temperature by powder X-ray diffraction (XRD) to confirm that the crystal retains this structure. As shown in Figure 5a, the diffraction peaks are intense and perfectly matched to the simple cubic structure ( $a = 10.59$  Å), in analogy to previously reported  $C_{70}$  microparticles.<sup>[36]</sup> This result implies that, at room temperature,  $C_{70}$  cubes have basically the same crystal structure as that at 90 K, with a slightly increased lattice constant. The intensity increases of the (001) and (002) peaks indicate that most  $C_{70}$  cubes make preferred surface contacts to the substrate through {001}-family planes. A transmission electron microscope (TEM) image and selected-area electron diffraction (SAED) data were also used to correlate each facet of the cube crystal to the plane of the simple cubic crystal structure. A clear electron-diffraction pattern appeared upon irradiation with an electron beam normal to the surface of a cube crystal (Figure 5b,c). The measured *d* spacing of the nearest and

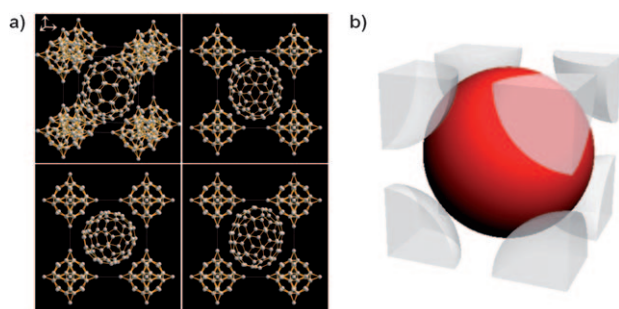


**Figure 4.** Crystal structure of  $C_{70}\cdot(\text{mesitylene})_2$ . a) Overall view of the unit cell (top left), and the unit cell viewed along the  $a$  (top right),  $b$  (bottom left), and  $c$  axes (bottom right). b) Schematic representation of the unit cell of the  $C_{70}\cdot(\text{mesitylene})_2$  cube crystal. The red sphere at the center and gray part spheres at each corner represent one  $C_{70}$  and two mesitylene molecules, respectively.

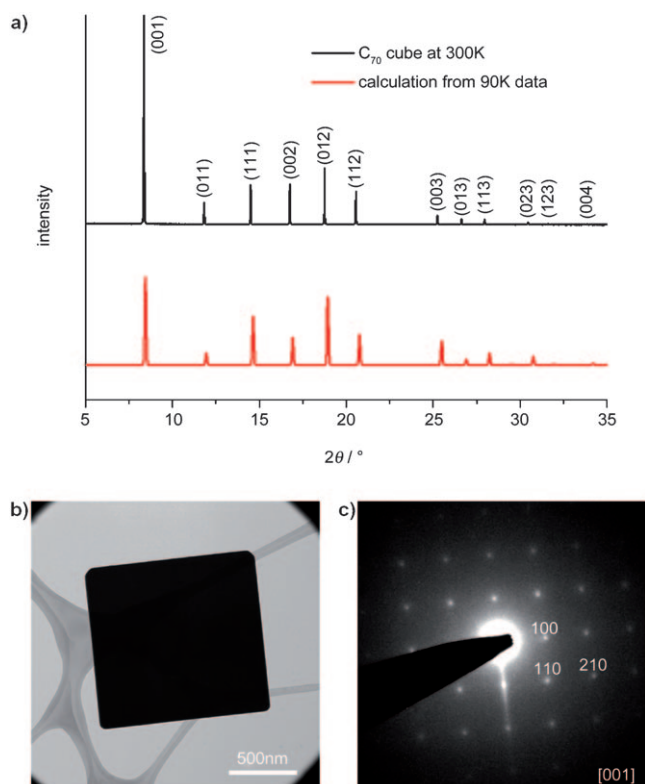


**Figure 5.** a) Powder X-ray diffraction patterns of a  $C_{70}$  cube, as measured at room temperature (black line) and calculated from single-crystal data obtained at 90 K (red line). Both spectra were matched to the wavelength of the  $\text{CuK}\alpha_1$  line ( $\lambda = 1.54056 \text{ \AA}$ ). b, c) TEM image of a  $C_{70}$  cube and corresponding electron-diffraction pattern ([001] zone axis).

second-nearest peaks to the center was 10.83 and 15.32  $\text{\AA}$ , respectively. These  $d$ -spacing values correspond well to (100) and (110) planes of a simple cubic crystal structure within 2.3 % error; hence, each facet of the  $C_{70}$  cube was confirmed to be a {100}-family plane. This conclusion agrees well with the results of powder XRD.

A unique characteristic of the  $C_{70}$  cubes is a remarkably enhanced photoluminescence (PL). Although many studies have revealed absorption and emission spectral changes

(peak shifts and peak broadening) of  $C_{70}$  aggregates formed either by simple precipitation or by the use of charge-transfer linkage molecules,<sup>[18,21]</sup> no such enormous PL enhancement has been reported. The  $C_{70}$  cubes were bright red in fluorescence microscope images ( $\lambda_{\text{ex}} = 510\text{--}560 \text{ nm}$ ,  $\lambda_{\text{em}} = 660\text{--}710 \text{ nm}$ ; Figure 6a), whereas no significant PL was observed from a  $C_{70}$  powder (Figure 6b). Figure 6c,d shows transmission optical microscope images of  $C_{70}$  cubes and a  $C_{70}$  powder, respectively.

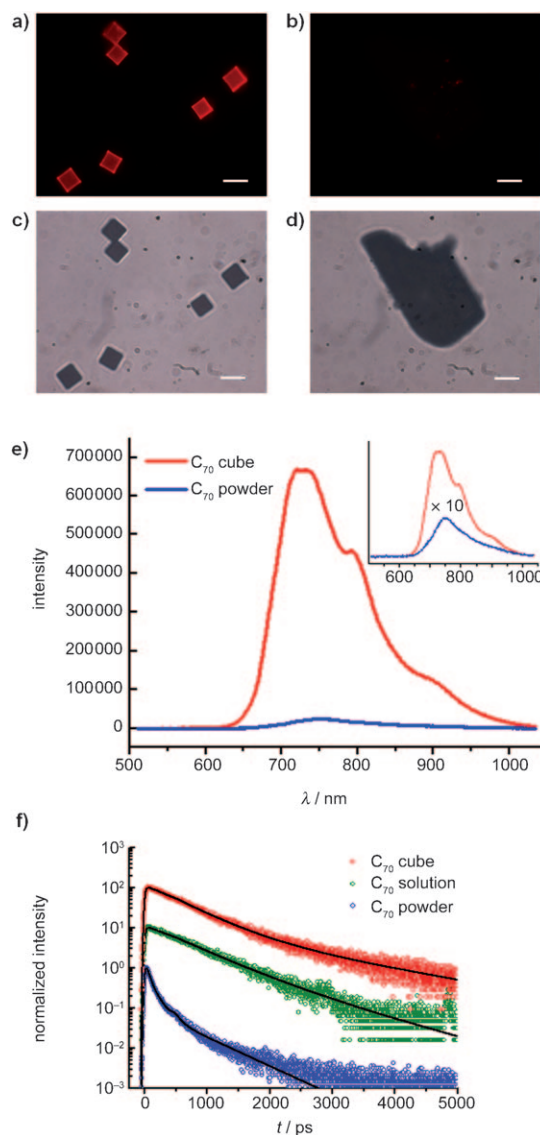


**Figure 6.** a), b) Fluorescence optical microscope images of  $C_{70}$  cubes and  $C_{70}$  powder, respectively. c), d) Transmission optical microscope images corresponding to (a) and (b), respectively. The scale bars in (a–d) are 10  $\mu\text{m}$ . e) PL spectra of  $C_{70}$  cubes (red) and  $C_{70}$  powder (blue). In the inset, the PL spectrum of the  $C_{70}$  powder has been increased by a factor of 10 for comparison. f) Time-resolved PL spectra measured at  $\lambda = 750 \text{ nm}$  ( $\lambda_{\text{ex}} = 400 \text{ nm}$ ). The time constants are 510 ps (91 %) and 1.6 ns (9 %) for the  $C_{70}$  cubes, 560 ps (85 %) and 1.1 ns (15 %) for  $C_{70}$  in solution, and 40 ps (45 %), 100 ps (50 %), and 610 ps (5 %) for the  $C_{70}$  powder. The spectra for the  $C_{70}$  cubes and  $C_{70}$  in solution are shifted by two orders and one order of magnitude, respectively, to enable clear comparison.

More-detailed information about the PL enhancement was obtained from PL spectra and time-resolved PL (TRPL) studies. The PL intensity of the  $C_{70}$  cubes was approximately 30 times higher than that of the  $C_{70}$  powder, even though an excess amount of the  $C_{70}$  powder was examined (Figure 6e). The PL spectrum of the  $C_{70}$  cubes is red-shifted slightly from that of the solution, as observed previously for  $C_{70}$  crystals.<sup>[37]</sup>

The enhancement of PL seems to be induced by the high crystallinity of the  $C_{70}$  cube, rather than by the influence of mesitylene molecules included in the crystal. To confirm this hypothesis, we prepared mesitylene-free  $C_{70}$  cubes by removing mesitylene molecules in an  $H_2$  atmosphere at 300 °C for 3 h. The resulting crystals retained the cube geometry as well as the PL intensity (see Figure S5 in the Supporting Information).

The direct influence of the high crystallinity of the  $C_{70}$  cubes on the PL enhancement was confirmed by the TRPL results. At 750 nm, the TRPL of the  $C_{70}$  cube decayed biexponentially with time constants of 510 ps (91 %) and 1.6 ns (9 %; Figure 6f, red circles). The main component can be assigned to the  $S_1$ – $S_0$  transition of a  $C_{70}$  molecule, as its time constant is close to the lifetime of the  $S_1$  state of an individual  $C_{70}$  molecule in solution.<sup>[38,39]</sup> That is, interactions between  $C_{70}$  molecules in the cube crystal may be negligible, so that fluorescence quenching, which is observed frequently in molecular aggregates, does not occur. On the other hand, the TRPL of  $C_{70}$  powder shows much faster decay, which is consistent with the much weaker fluorescence intensity of the powder. This faster decay is possibly due to increased nonradiative relaxation through coupling between  $C_{70}$  molecules. Note that this interpretation is different from the aggregation-induced (crystallization-induced) emission mainly caused by the restriction of intramolecular rotations;<sup>[12–15]</sup> an effect that is absent in  $C_{70}$ .

In summary,  $C_{70}$  molecules undergo spontaneous self-crystallization into cube crystals in a precipitation process in solvent mixtures containing mesitylene and IPA as a good and a poor solvent, respectively. After optimization of the composition of the solvent and the concentration of  $C_{70}$ , and with the use of ultrasonication, we obtained  $C_{70}$  cube crystals with sharp edges, clean surfaces, and a homogeneous size distribution. The crystal structure has a simple cubic unit cell with a lattice constant of 10.47 Å at 90 K and 10.59 Å at room temperature; thus, the unit cell is composed of one  $C_{70}$  and two mesitylene molecules.  $C_{70}$  cube crystals emit remarkably increased PL as a result of the substantially increased crystallinity of  $C_{70}$  together with the decreased interactions between  $C_{70}$ , so that optical quenching is suppressed. Our results provide great opportunities for the fundamental understanding of the formation of various  $C_{70}$  self-crystallized architectures in simple solvent mixtures with specific combinations of solvents. Moreover, new  $C_{70}$  architectures with unprecedented optical properties will boost the development of organic-molecule-based optoelectronic devices for diverse applications.

## Experimental Section

**Synthesis of  $C_{70}$  cube crystals by precipitation:** The starting  $C_{70}$ /mesitylene solution was prepared by mixing  $C_{70}$  powder (MER Corporation, 95 %) and mesitylene (Sigma–Aldrich, 98 %), followed by ultrasonication for 30 min.  $C_{70}$ /mesitylene solutions with concentrations of 0.1, 0.2, and 0.4 mg mL<sup>−1</sup> were used. Isopropyl alcohol (IPA) was added to the vial containing the  $C_{70}$ /mesitylene solution, and the mixture was subjected to ultrasonication for the first 30 s. The final mixture was maintained at room temperature for 24 h. The initially dark purple color of the  $C_{70}$ /mesitylene solution became lighter after the addition of IPA. As precipitation occurred, the final solution lost its original color and became transparent. It took several hours for the precipitates to settle at the bottom of the vial. The precipitates were transferred onto a precleaned Si or quartz substrate for characterization.

**Synthesis of large  $C_{70}$  cube crystals by liquid–liquid diffusion:** IPA was added slowly along the wall of a vial containing the  $C_{70}$ /mesitylene solution so that the two liquids could form a clear interface. Over 5 days, both liquid layers slowly diffused into each other and merged to form a homogeneous mixture, and large  $C_{70}$  cube crystals were formed on the bottom of the vial. The crystals were transferred onto a glass slide with a pipette and placed in the single-crystal X-ray diffractometer by using a microneedle. Full-sphere data sets were collected by using a Bruker APEX II QUAZAR instrument in house and the ADSC Quantum 210 detector system in the 6B2 beamline of the Pohang Accelerator Laboratory.

**Structure characterization:** A JEOL JSM-7401F instrument was used for SEM imaging. A JEOL JEM3010 instrument was used with an acceleration voltage of 300 kV for recording TEM images and electron-diffraction patterns. Powder X-ray diffraction data were collected by using a synchrotron (Pohang Accelerator Laboratory, 5C2 beamline) X-ray source with a radiation wavelength of 1.23956 Å.

Received: August 12, 2010

Published online: November 9, 2010

**Keywords:** cube crystals · fullerenes · photoluminescence · self-crystallization · solvent effects

- [1] J. G. C. Veinot, T. J. Marks, *Acc. Chem. Res.* **2005**, *38*, 632–643.
- [2] S. R. Forrest, *Nature* **2004**, *428*, 911–918.
- [3] L. Zang, Y. Che, J. S. Moore, *Acc. Chem. Res.* **2008**, *41*, 1596–1608.
- [4] D. O'Carroll, I. Lieberwirth, G. Redmond, *Nat. Nanotechnol.* **2007**, *2*, 180–184.
- [5] S. Liu, W. M. Wang, A. L. Briseno, S. C. B. Mannsfeld, Z. Bao, *Adv. Mater.* **2009**, *21*, 1217–1232.
- [6] M. Steinhart, J. H. Wendorff, A. Greiner, R. B. Wehrspohn, K. Nielsch, J. Schilling, J. Choi, U. Gösele, *Science* **2002**, *296*, 1997.
- [7] R. C. Haddon, L. E. Brus, K. Raghavachari, *Chem. Phys. Lett.* **1986**, *125*, 459–464.
- [8] R. C. Haddon, *Acc. Chem. Res.* **1992**, *25*, 127–133.
- [9] A. F. Hebard, M. J. Rosseinsky, R. C. Haddon, D. W. Murphy, S. H. Glarum, T. T. M. Palstra, A. P. Ramirez, A. R. Kortan, *Nature* **1991**, *350*, 600–601.
- [10] Y. P. Sun, P. Wang, N. B. Hamilton, *J. Am. Chem. Soc.* **1993**, *115*, 6378–6381.
- [11] M. R. Han, Y. Hirayama, M. Hara, *Chem. Mater.* **2006**, *18*, 2784–2786.
- [12] Y. Hong, J. W. Y. Lam, B. Z. Tang, *Chem. Commun.* **2009**, 4332–4353.
- [13] B. K. An, S. K. Kwon, S. D. Jung, S. Y. Park, *J. Am. Chem. Soc.* **2002**, *124*, 14410–14415.

- [14] Y. Dong, J. W. Y. Lam, A. Qin, Z. Li, J. Sun, H. H. Y. Sung, I. D. Williams, B. Z. Tang, *Chem. Commun.* **2007**, 40–42.
- [15] L. Qian, B. Tong, J. Shen, J. Shi, J. Zhi, Y. Dong, Y. Dong, J. W. Y. Lam, Y. Liu, B. Z. Tang, *J. Phys. Chem. B* **2009**, *113*, 9098–9103.
- [16] M. Baibarac, L. Mihut, N. Preda, I. Baltog, J. Y. Mevellec, S. Lefrant, *Carbon* **2005**, *43*, 1–9.
- [17] H. N. Ghosh, A. V. Sapre, J. P. Mittal, *J. Phys. Chem.* **1996**, *100*, 9439–9443.
- [18] A. M. Husanu, I. Baltog, M. Baibarac, N. Preda, L. Mihut, T. Velula, C. Bucur, *Rom. J. Phys.* **2009**, *54*, 529–538.
- [19] Y. P. Sun, C. E. Bunker, *Nature* **1993**, *365*, 398.
- [20] S. Nath, H. Pal, A. V. Sapre, *Chem. Phys. Lett.* **2002**, *360*, 422–428.
- [21] M. Alfè, B. Apicella, R. Barbella, A. Bruno, A. Ciajolo, *Chem. Phys. Lett.* **2005**, *405*, 193–197.
- [22] S. Pekker, É. Kováts, G. Oszlányi, G. Bényei, G. Klupp, G. Bortel, I. Jalsovszky, E. Jakab, F. Borondics, K. Kamarás, M. Bokor, G. Kriza, K. Tompa, G. Faigel, *Nat. Mater.* **2005**, *4*, 764–767.
- [23] M. Sathish, K. Miyazawa, *J. Am. Chem. Soc.* **2007**, *129*, 13816–13817.
- [24] L. Wang, B. Liu, D. Liu, M. Yao, Y. Hou, S. Yu, T. Cui, D. Li, G. Zou, A. Iwasiewicz, B. Sundqvist, *Adv. Mater.* **2006**, *18*, 1883–1888.
- [25] C. Park, H. J. Song, H. C. Choi, *Chem. Commun.* **2009**, 4803–4805.
- [26] J. Geng, W. Zhou, P. Skelton, W. Yue, I. A. Kinloch, A. H. Windle, B. F. G. Johnson, *J. Am. Chem. Soc.* **2008**, *130*, 2527–2534.
- [27] H. S. Shin, S. M. Yoon, Q. Tang, B. Chon, T. Joo, H. C. Choi, *Angew. Chem.* **2008**, *120*, 705–708; *Angew. Chem. Int. Ed.* **2008**, *47*, 693–696.
- [28] K. Miyazawa, *J. Am. Chem. Soc.* **2002**, *85*, 1297–1299.
- [29] K. Miyazawa, J. Minato, T. Yoshii, M. Fujino, T. Suga, *J. Mater. Res.* **2005**, *20*, 688–695.
- [30] P. A. Troshin, V. V. Prisyazhnuk, S. I. Troyanov, O. V. Boltalina, Y. A. Ma, *Electrochem. Soc. Proc.* **2001**, 548–558.
- [31] P. Müller, *Crystallogr. Rev.* **2009**, *15*, 57–83.
- [32] K. Miyazawa, Y. Kuwasaki, A. Obayashi, M. Kuwabara, *J. Mater. Res.* **2002**, *17*, 83–88.
- [33] R. M. Fleming, T. Siegrist, P. M. Marsh, B. Hessen, A. R. Kortan, D. W. Murphy, R. C. Haddon, R. Tycko, G. Dabbagh, A. M. Mulsce, M. L. Kaplan, S. M. Zahurak, *Mater. Res. Soc. Symp. Proc.* **1991**, *206*, 691–695.
- [34] Crystallographic data for the  $C_{70}$  cube crystal:  $C_{88}H_{24}$ , MW = 1087.12, cubic, space group  $P43m$ ,  $\lambda(Mo_{K\alpha}) = 0.71073 \text{ \AA}$ ,  $T = 90(1) \text{ K}$ ,  $a = b = c = 10.4774(8) \text{ \AA}$ ,  $V = 1150.2(2) \text{ \AA}^3$ ,  $Z = 1$ ,  $d_{\text{calcd}} = 1.570 \text{ mgm}^{-3}$ . Isotropic least-squares refinement (24 parameters) on 267 independent merged reflections ( $R_{\text{int}} = 0.0297$ ) converged at  $R_1(F) = 0.1989$  for 161 observed data points ( $I > 2\sigma(I)$ ), GOF = 2.897. The occupancy factors of  $C_{70}$  and two mesitylene molecules are 0.04167, 0.150, and 0.150, respectively. CCDC 769202 contains the supplementary crystallographic data for this paper. These data can be obtained free of charge from The Cambridge Crystallographic Data Centre via [www.ccdc.cam.ac.uk/data\\_request/cif](http://www.ccdc.cam.ac.uk/data_request/cif).
- [35] The second-best space-group candidate was  $Pm\bar{3}m$ . However, we could not solve the structure with  $Pm\bar{3}m$ .
- [36] K. Matsuoka, T. Akiyama, S. Yamada, *Langmuir* **2010**, *26*, 4274–4280.
- [37] M. Ichida, M. Sakai, T. Yajima, A. Nakamura, H. Shinohara, *Chem. Phys. Lett.* **1997**, *271*, 27–32.
- [38] D. Kim, M. Lee, *J. Am. Chem. Soc.* **1992**, *114*, 4429–4430.
- [39] S. K. Lin, L. L. Shiu, K. M. Chien, T. Y. Luh, T. I. Lin, *J. Phys. Chem.* **1995**, *99*, 105–111.